

# Preparation and Characterization of HAP/Carboxymethyl Chitosan Nanocomposites

B. Sreedhar,<sup>1</sup> Y. Aparna,<sup>1</sup> M. Sairam,<sup>2</sup> Neha Hebalkar<sup>1</sup>

<sup>1</sup>*Inorganic and Physical Chemistry Division, Indian Institute of Chemical Technology, Tarnaka, Hyderabad 500 007, India*

<sup>2</sup>*Center of Excellence in Polymers Science, Karnatak University, Dharwad 580 003, India*

Received 23 June 2006; accepted 10 January 2007

DOI 10.1002/app.26140

Published online 6 April 2007 in Wiley InterScience (www.interscience.wiley.com).

**ABSTRACT:** Nanocomposites of modified chitosan, carboxymethyl chitosan (CMCh) with hydroxyapatite (HAP) have been prepared by coprecipitation technique. Totally three nanocomposites containing 80/20, 50/50, and 20/80 of HAP/CMCh have been prepared and were characterized by using transmission electron microscopy (TEM), X-ray diffraction (XRD), fourier transformed infrared spectroscopy (FTIR), X-ray photoelectron spectroscopy (XPS), thermogravimetry (TG), and scanning electron microscopy (SEM). Modified chitosan, CMCh, which is water soluble can be used for drug delivery application. TEM micrographs of the nanocomposites revealed the formation of

small HAP crystallites of about 230 nm in length and 30 nm in width that are aggregated to form elliptical shapes or morphology. TGA thermograms showed that the thermal stability of the CMCh increased with incorporation of HAP. FTIR, XRD, and XPS analysis of CMCh/HAP nanocomposites showed the peaks corresponding to CMCh as well as HAP and confirm the formation of HAP/CMCh nanocomposites. © 2007 Wiley Periodicals, Inc. *J Appl Polym Sci* 105: 928–934, 2007

**Key words:** hydroxyapatite; carboxymethyl chitosan; water soluble; nanocomposite

## INTRODUCTION

In recent years significant research effort has been devoted to organic-inorganic nano-composites because of their potential application in biology, electronics, and optical technology. Calcium hydroxyapatite (HAP)  $[(Ca_{10}(PO_4)_6(OH)_2)]$  is an important material because of its high thermal stability, unique sorption properties and biocompatibility. HAP is an important biomaterial used in hard tissue surgery because of its bioactive nature.<sup>1–3</sup> It can be used as biocompatible and osteoconductive substitute in the field of orthopedic surgery, immediate tooth replacement, pulp-capping material, repair of bone defects etc.<sup>4</sup> Experiments are performed on the study of slow releasing anticancer drug implantation treatment as a new therapy for hepatocellular carcinoma. HAP was chosen as the carrier material for doxorubicin hydrochloride (DOX), an anticancer agent.<sup>5</sup> DOX-HAP was produced by adsorbing DOX on porous HAP particles of 1375  $\mu$ m diameter using the freeze drying method. These experiments showed the steady release of DOX from HAP for one month duration. Calcium HAP is a complete bone building food and can help to reduce bone

loss and is the most easily absorbed calcium source. However, this ceramic is difficult to shape up in required form because of its hardness or brittleness. This problem can be solved by making nano-composites of calcium HAP with modified chitosan. Chitosan is made up of *N*-deacetylglucosamine units linked through 1–4 glycosidic bonds. The most important property of chitosan is its biodegradability. Chitosan degrades in the body as nonharmful and nontoxic compounds without causing any damage to human body. Nanocomposites of chitosan/HAP have been prepared and are found to show increased osteoconductivity and biodegradation for orthopedic use. The effect of citric acid on chitosan/HAP nanocomposites was studied.<sup>6</sup> TEM pictures of the nanocomposites revealed the formation of ordered elliptic particles of chitosan with HAP crystallites. The mechanical properties of the chitosan/HAP composites were enhanced upon addition of a small amount of citric acid.<sup>6</sup> Citric acid enlarged the precipitate size of chitosan/HAP composites, through interactions with chitosan rather than HAP.

Paste made from chitosan glutamate and HAP was used to deliver osteoinductive factors like bone-marrow aspirate, or BMP-2, or osteoblasts cultured from the bone-marrow aspirate. The bone-mineral density and histology data indicated that the paste containing osteoblasts cultured from bone-marrow aspirate would form mineralized bone. Among the other osteoinductive agents tested here, BMP-2 also showed

Correspondence to: B. Sreedhar (sreedharb@iict.res.in).

Contract grant sponsor: Science Engineering and Research Council (SERC), India.

*Journal of Applied Polymer Science*, Vol. 105, 928–934 (2007)  
© 2007 Wiley Periodicals, Inc.

 **WILEY**  
**InterScience®**  
DISCOVER SOMETHING GREAT

the osteoblastic activity. No untoward reaction was seen in any of the groups; hence, the paste of chitosan glutamate and HAP was found to be an effective vehicle to deliver different biomolecules for bone ingrowth.<sup>7</sup> Nanosized HAP powder of 20–30 nm in width and 50–60 nm in length was synthesized. The specific surface area of the powder is 73.0 m<sup>2</sup>/g. HAP/chitosan nanocomposites were prepared by precipitating the nano sized particles. The particles were of homogeneous microstructure that will be helpful to produce uniform nanomaterial. It was proposed that the nanostructure of HAP/chitosan composite has the best biomedical properties in the biomaterials applications.<sup>8</sup> Chitosan/HAP membranes were developed and used in guided tissue regeneration and for the limitation of HAP particle migration at sites of implantation.<sup>9</sup> It was found that the ratio of HAP to chitosan sol of 4/11 by weight was optimal for preparation of a composite membrane that can be of value in guided tissue regeneration and in localizing HAP at implantation sites in periodontal bony defects or over extensively resorbed edentulous alveolar ridges. Histologic evaluation revealed that the composite membranes were biologically well tolerated, with fibrous encapsulation and occasional osteogenesis extending into the connective tissue that surrounded the implant. Increasing the HAP content seemed to enhance membrane degradation.<sup>9</sup> Self-hardening paste was made by using a combination of chitosan, HAP, ZnO, and CaO. The strength of the chitosan-HAP hardened composite was comparable with that of the cancellous bone derived from tibial eminentia, but was considerably lower than that of PMMA bone cement.<sup>10</sup> Novel nanohydroxyapatite/chitosan composite scaffold with high porosity was developed.<sup>11</sup> The nano-HAP particles were made *in situ* through a chemical method and dispersed well on the porous scaffold. The composite scaffolds showed better biocompatibility than pure chitosan scaffolds. The results suggest that the newly developed nano-HAP/chitosan composite scaffolds may serve as a good three-dimensional substrate for cell attachment and migration in bone tissue engineering.

In addition to biodegradation, chitosan is having wound healing property and can be used as antibacterial agent. Chitosan is flexible and has a high resistance upon heating because of the intra molecular hydrogen bonds formed between hydroxyl and amino groups. Chitosan was found to enhance the permeability of intestinal and nasal epithelia by opening the tight junction between cells, thereby favoring paracellular drug transport. Chitosan is polycationic in nature and dissolves in solution containing aqueous acids. Even though chitosan is readily soluble in aqueous acid solution, it is intractable to any organic solvent or thermo processing technique because of its stout crystalline structures.<sup>12</sup> Many efforts were made to improve the

solubility and meltability of chitosan because of its wider utilization as biopolymer. The water soluble derivative has been used as starting material for the chemical modification of chitosan, as a substrate for chitinase and chitosanase and as ecological and environmentally friendly materials in agriculture, biomedical, cosmetic, and food additive fields.<sup>13</sup> In the present study, to improve the solubility of chitosan (to make it soluble in water), chitosan is modified as carboxymethyl chitosan (CMCh). CMCh is a polyanion derivative of chitosan and soluble in water at pH = 7. CMCh is of particular interest because it was proved to behave as an intestinal absorption enhancer.<sup>14</sup>

A search of literature indicated that no previous reports on nanocomposites of HAP with water soluble CMCh. In the present study, a water soluble chitosan derivative, carboxymethyl chitosan (CMCh) was prepared and this modified derivative of chitosan was used for the preparation of nanocomposites with HAP because of its potential application in various fields. HAP/CMCh nano-composites (80/20, 50/50, and 20/80) were prepared by coprecipitation method and sonicated for 1 h to get homogeneous nanocomposite. These nano-composites were characterized by transmission electron microscopy (TEM), thermogravimetry (TG), Fourier-transformed infrared spectroscopy (FTIR), X-ray photoelectron spectroscopy, X-ray diffraction (XRD) and scanning electron microscopy (SEM) and the results are presented.

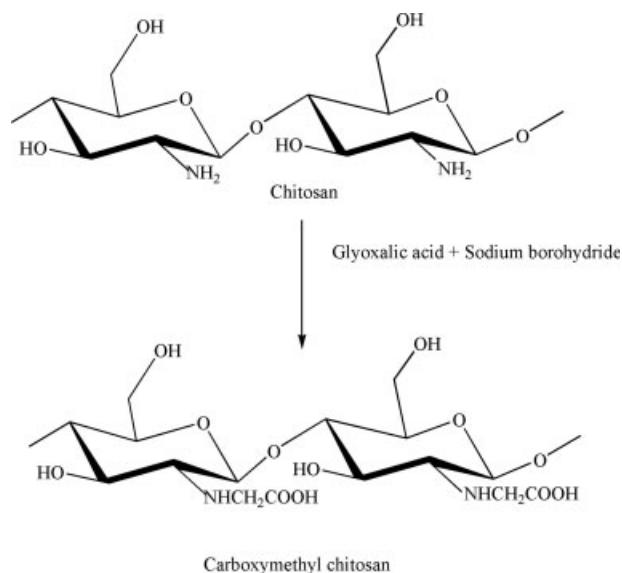
## EXPERIMENTAL

### Materials

Chitosan and analytical grade Ca(OH)<sub>2</sub>, H<sub>3</sub>PO<sub>4</sub>, acetic acid, sodium borohydride were procured from Aldrich, USA and were used without further purification. Glyoxylic acid was purchased from Acros (India).

### Preparation of CMCh

CMCh was prepared by the method reported by Di Colo et al. and was slightly modified.<sup>14</sup> The procedure for modification is as follows: 1.5 g of chitosan was dissolved in 0.7% aqueous acetic acid solution by stirring. After 30 min, 2.7 g of glyoxylic acid was added and stirred at ambient temperature for 90 min. Then pH of solution was brought down to 4.5 by adding of 0.1M NaOH over 30 min. After that stirring was continued for further 45 min. The above solution was reduced by adding an aqueous solution of sodium borohydride [5% (w/v)]. This mixture was stirred at ambient temperature for 1 h. The polymer was precipitated by adding excess ethanol and was collected by filtration under vacuum. The same procedure was repeated with the filtered material and this filtered material was used as starting material for the second



**Scheme 1** Preparation of carboxymethyl chitosan.

step. The final product obtained by this method was used for the preparation of HAP/CMCh nanocomposites. The modification procedure is as described in Scheme 1.

### ***In situ* preparation of HAP/CMCh nanocomposites**

Various synthesis methods were used in literature for the preparation of HAP/chitosan nanocomposites. In the present study HAP/CMCh (80/20, 50/50, and 20/80 (wt/wt) nano-composites were prepared by coprecipitation method.<sup>3</sup> CMCh aqueous solution was prepared by dissolving CMCh powder in distilled water. Then  $H_3PO_4$  (8.5 wt %) solution was added to CMCh solution and sonicated for 30 min.  $Ca(OH)_2$  solution was added to CMCh solution drop by drop during sonication and sonication continued for another 1 h. HAP/CMCh nanocomposite was precipitated and this solution was left for aging for 24 h in stirring. The nano-composites so formed were characterized by TGA, XPS, XRD, FTIR, TEM, and SEM techniques.

### **Characterization**

**Thermogravimetric analysis (TGA, DTG)**

Thermogravimetric measurements (TGA) were carried out on Mettler Toledo TGA/SDTA 851<sup>e</sup> thermal system (Zurich, Switzerland) from 25 to 800°C in  $N_2$  environment (flow rate, 20 mL/min) at a heating rate of 20°C/min. The sample size was in between 10 and 12 mg.

**Transmission electron microscopy**

FEI Tecnai F12 (Philips Electron Optics, Holland), operated at 100 kV, was used to study and record the

TEM images. The samples were dispersed in methanol and a drop of the dispersed liquid was placed and dried on polymer coated copper grid.

**Scanning electron microscopy**

Morphology studies of CMCh composites were carried out using Hitachi S520 scanning electron microscope.

**Fourier transformed infrared Spectroscopy**

Fourier transform IR spectra (FTIR) of the CMCh and its nanocomposites were obtained using a Thermo Nicolet Nexus 670 spectrometer in the region 4000–400  $cm^{-1}$ .

**X-ray diffraction**

X-ray diffraction spectra of HAP/CMCh nanocomposites were recorded using Siemens/D-5000 X-ray diffractometer using  $CuK_{\alpha}$  radiation of wave length 1.54 Å and continuous speed of 0.045°/min.

**X-ray photoelectron spectroscopy**

X-ray photoemission spectra were recorded on a KRATOS AXIS 165 with a dual anode (Mg and Al) apparatus using the Mg  $K_{\alpha}$  anode. The pressure in the spectrometer was about  $10^{-9}$  Torr. For energy calibration we have used the carbon 1 s photoelectron line. The carbon 1 s binding energy was taken to be 284.6 eV. Spectra were deconvoluted using Sun Solaris based Vision 2 curve resolver. The location and the full width at half maximum (FWHM) for a species was first determined using the spectrum of a pure sample. The location and FWHM of products, which were not obtained as pure species, were adjusted until the best fit was obtained. Symmetric Gaussian shapes were used in all cases. Binding energies for identical samples were, in general, reproducible to within  $\pm 0.1$  eV.

## **RESULTS AND DISCUSSION**

### **Thermogravimetry**

The organic composition of the nano-composite was determined with thermo-gravimetric analysis carried out in the temperature range 20–800°C at a heating rate of 20°C/min in  $N_2$  atmosphere. Figure 1 shows TGA-DTG curves of pure chitosan, CMCh, and various HAP/CMCh nano-composite concentrations (80/20, 50/50, and 20/80). The thermal stability of CMCh is lower than that of the pure chitosan. However, the incorporation of HAP into chitosan improved the thermal stability of the CMCh because of the formation of HAP/CMCh composite. From the

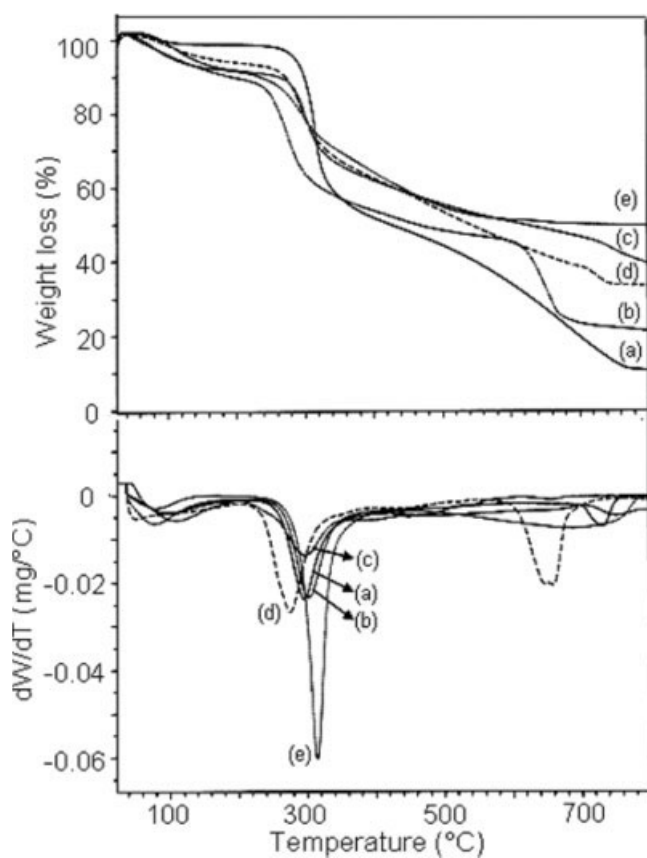


**Figure 1** TGA-DTG thermograms of (a) chitosan, (b) CMCh and various HAP/CMCh nanocomposites (c) 80/20, (d) 50/50, (e) 20/80.

thermograms it is clear that the thermal stability of nano-composites increased with increasing HAP content in the nano-composites. As the HAP content increased, the onset of degradation of CMCh showed a shift from 259 to 281°C. Thermograms of nano-composites and CMCh indicated two stage weight loss in which, first stage corresponds to loss of water whereas the second stage is due to the decomposition of CMCh. It was observed that the sample weight rapidly decreased with increasing temperature, especially in the ranges 40–130°C and 250–600°C. A broad

endothermic peak observed at 80°C is assigned to the loss of water and exothermic peak at 320°C is ascribed to the thermal decomposition of CMCh.<sup>15</sup> Considering the CMCh structure, water molecules can be bound by two polar groups, hydroxyl and amine, present in this macromolecule. FTIR studies suggested that the interaction of water with hydroxyl groups is stronger than amine groups.<sup>16</sup> In our studies considerable amount of water removal from chitosan occurred below 100°C. It is due to the association of water molecules with the amine and hydroxyl groups of chitosan. The weight loss in second stage is due to decomposition of chitosan. From literature it is clear that pyrolysis of polysaccharides starts by a random split of the glycosidic bonds followed by a further decomposition forming acetic and butyric acids and a series of lower fatty acids.<sup>17</sup> The CMCh content in the composite was determined from the weight loss in the temperature range 200–600°C. The compositions calculated from Figure 1 are in good agreement with the initial compositions taken for the preparation of HAP/CMCh nanocomposites.

#### Transmission electron microscopy

The TEM micrographs of pure HAP and HAP/CMCh (50/50) nano-composites are shown in Figure 2. The TEM micrograph of HAP shows [Fig. 2(a)] the formation of small crystallites of uniform size without much aggregation. The size of the particles calculated from TEM micrograph shows that the particles are elongated and are about 230 nm in length and 30 nm in width. The crystallinity of HAP grains and grain boundaries suggested that the material has an excellent phase homogeneity and purity. The micrograph of nano-composite [Fig. 2(b)] indicated both CMCh and HAP. Many elliptical aggregations consisting of small HAP crystallites were observed.

#### Scanning electron microscopy

The scanning electron micrographs of pure HAP and HAP/CMCh (50/50) nano-composites are shown in

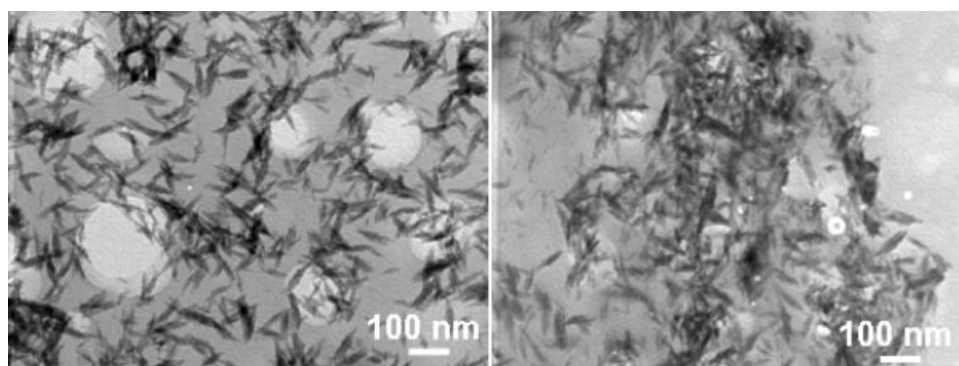


**Figure 2** Transmission electron micrographs of (a) pure HAP and (b) HAP/CMCh (50/50).

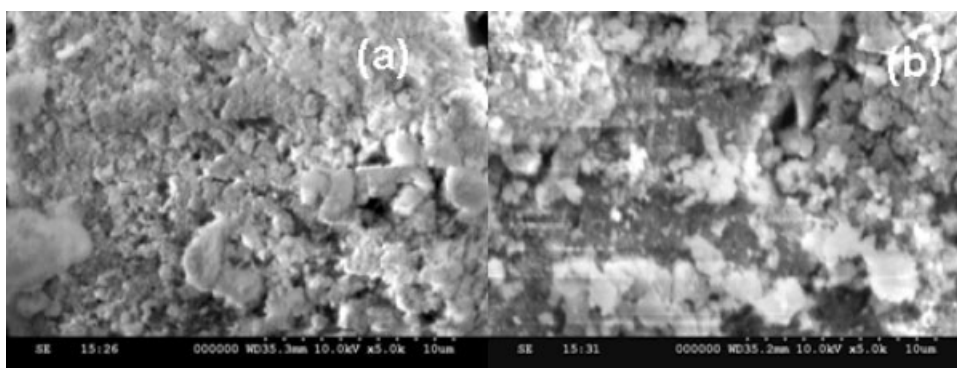


**Figure 3** Scanning electron micrographs of (a) pure HAP and (b) HAP/CMCh (50/50).

Figure 3. SEM image of pure HAP indicated the presence of many agglomerations leaving submicrometric pores in between. The formation of pores is beneficial because these pores will permit the circulation of physiological fluid throughout the coating when it is used as biomaterial. Morphological studies of nanocomposites (HAP/CMCh) revealed the presence of both HAP and CMCh. SEM micrographs of nanocomposites showed nano-size character, which then aggregates forming the micrometric aggregates.

#### FTIR analysis

The FTIR spectra of CMCh and HAP/CMCh nanocomposites (80/20, 50/50, and 20/80) are shown in Figure 4. IR spectra were recorded in the range 4000–400  $\text{cm}^{-1}$ . The FTIR spectrum of HAP indicated absorption bands at 3441, 1041, 873, 604, and 568  $\text{cm}^{-1}$ . The absorption band at 3441  $\text{cm}^{-1}$  is due to OH group and bands at 1041, 560–630  $\text{cm}^{-1}$  are due to  $\text{PO}_4^{-3}$  in HAP. The absorption band at 873  $\text{cm}^{-1}$  is attributed to the presence of  $\text{CO}_3^{-2}$  group. The FTIR spectrum of CMCh indicated absorption bands at 3443, 1628  $\text{cm}^{-1}$  because of  $\text{NH}_2$  group and bands at 2924, 2854  $\text{cm}^{-1}$  corresponding to the presence of C–H bond of chitosan. Absorption bands present at 1449 and 1370  $\text{cm}^{-1}$  are due to the presence of bending of C–H bonds. FTIR spectra of HAP/CMCh nanocomposites showed characteristic absorption bands of both HAP and CMCh. The absorption bands at 3439, 1629, and 1415 indicated the presence of CMCh in the nanocomposites. The absorption bands observed at 1041, 604, 568  $\text{cm}^{-1}$  are due to phosphate groups of HAP in the nano-composite. FTIR data clearly confirmed the formation of HAP/CMCh nanocomposites.

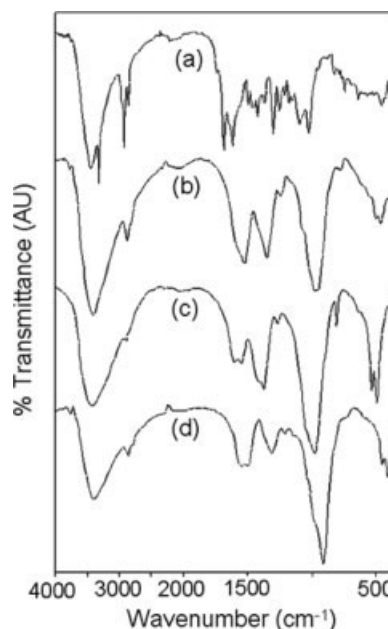
#### XRD analysis

Figure 5 shows X-ray diffractograms of pure HAP and HAP/CMCh (80/20) nano-composite. XRD spectrum of pure HAP indicated very sharp peaks at  $2\theta$

$= 34^\circ$ ,  $47^\circ$ , and  $51^\circ$ . These peaks are attributed due to, (202), (222), and (213) orientations, respectively.<sup>3</sup> Both HAP and CMCh peaks observed in the XRD pattern of nano-composites of HAP/CMCh. The peak found at  $2\theta = 20^\circ$  was assigned to chitosan chains (Chen et al.<sup>8</sup>). The other XRD peaks at  $2\theta = 34^\circ$ ,  $47^\circ$  are characteristic of (202), (222) orientations indicating the presence of HAP in nanocomposites. XRD data confirmed the formation of HAP/CMCh nanocomposites.

#### XPS analysis

XPS is an important surface sensitive analytical technique useful for the identification of elements present in nano-composites. XPS also gives stoichiometric information of the constituent elements present in the nano-composite and the chemical environment



**Figure 4** FTIR spectra of (a) CMCh and HAP/CMCh nanocomposites (b) 80/20, (c) 50/50, and (d) 20/80.

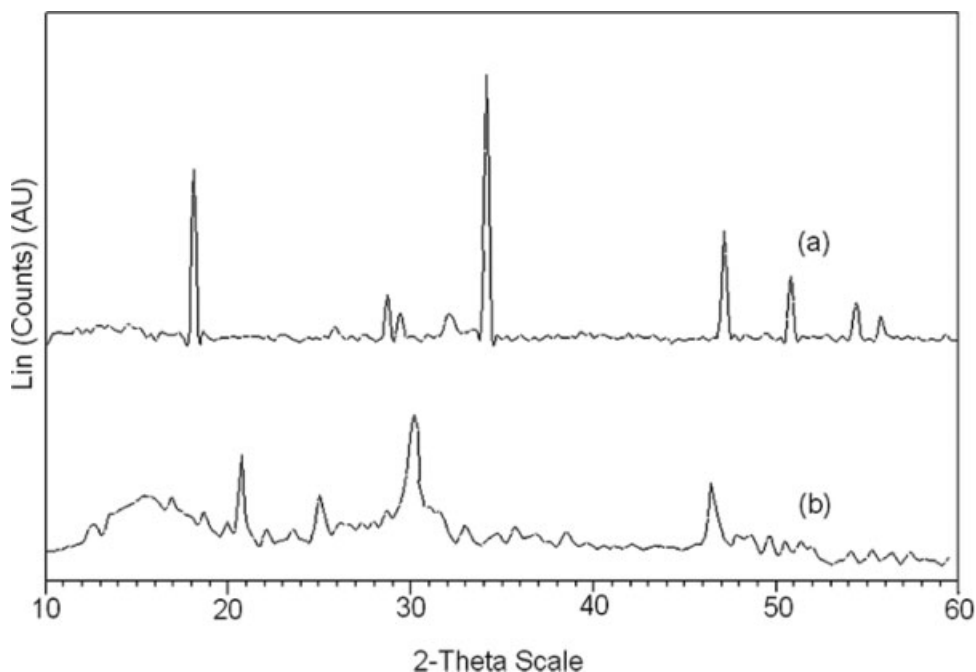


**Figure 5** X-ray diffractograms of (a) HAP and (b) HAP/CMCh nanocomposite (80/20).

around the elements. Figure 6 shows the XPS survey scans of CMCh and HAP/CMCh (50/50) nanocomposite. XPS survey spectrum of CMCh shows peaks characteristic of carbon, nitrogen and oxygen which are due to elements in modified chitosan (CMCh). On the other hand the survey spectrum of nano-composites showed peaks due to calcium and phosphate in addition to carbon, oxygen, nitrogen indicating the nano-composite formation. The peak observed at 133.9 eV is attributed due to phosphate (P 1s) and the binding energy peaks at 347.5 eV and 351.1 eV are characteristic of calcium, Ca 2p<sub>3/2</sub> and Ca 2p<sub>1/2</sub> respectively. The carbon peaks of chitosan, CMCh, HAP/CMCh nano-composites for various concentrations (80/20, 50/50, and 20/80) are compared in Figure 7. The deconvolution of carbon peak C 1 s indicated four

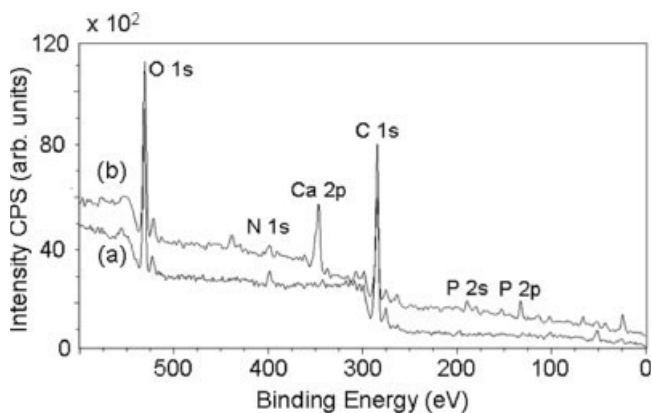


**Figure 6** X-ray photoelectron survey scans of (a) CMCh and (b) HAP/CMCh (50/50) nanocomposite.

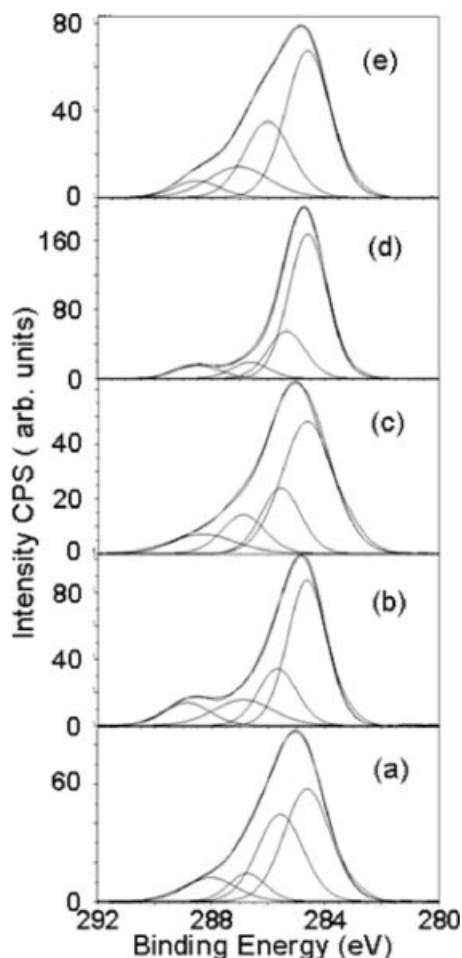


**Figure 7** XPS high resolution narrow scans of carbon 1s (a) chitosan, (b) CMCh, (c) 80/20, (d) 50/50 and (e) 20/80.

components of carbon. The carbon peak at binding energy 284.6 eV is due to the presence of C—C bond and peak at 285.12 eV is assigned to C—N bond. The peaks at binding energies 286.6 and 288.5 eV are attributed to the presence of C—O and C=O respectively. The presence of these bonds is also confirmed by deconvolution of oxygen peaks. Peak fitting of O indicated two peaks at binding energies 531.6 and 532.6 eV confirming the presence of C—O and C=O bonds. Nitrogen binding energy peak was observed at 400.3 eV which is due to N 1s indicating the presence of C—N bond. The XPS results of chitosan and CMCh were compared and all bonds afore mentioned were present in both chitosan and CMCh. The results are in good agreement with literature value.<sup>18</sup> XPS data clearly indicates the presence of HAP and CMCh in nano-composites which clearly confirms the nano-composite formation.

### CONCLUSIONS

Chitosan is modified as CMCh using standard method to make it soluble in water at pH = 7. Novel composites of HAP/CMCh (ratios with 80/20, 50/50, and 20/80) were prepared by coprecipitation method. HAP/CMCh nanocomposites were characterized by XRD, TGA, XPS, FTIR, TEM, and SEM analytical techniques. The morphological studies indicated that HAP crystallites were in the nano-range and the size of the crystallites is about 230 nm in length and 30 nm in width. FTIR studies indicated functional groups of both chitosan and HAP confirming the formation of nanocomposites. From TG studies it was established that the thermal stability of nano-composite increased with increasing HAP content in the nano-composites. XRD and XPS data indicated the characteristic peaks

of CMCh and HAP and confirmed the formation of HAP/CMCh nano-composites.

### References

1. Bose, S.; Saha, S. K. *Chem Mater* 2003, 15, 4464.
2. Matsuda, A.; Ikoma, T.; Kobayashi, A.; Tanaka, J. *Mater Sci Eng C* 2004, 24, 723.
3. Yamaguchi, I.; Tokuchi, K.; Fukuzaki, H.; Koyama, Y.; Takakuda, K.; Monma, H.; Tanaka, J. *J Biomed Mater Res* 2001, 55, 20.
4. Kriakose, T. A.; Narayana, S. K.; Palanichamy, M.; Arivuoli, D.; Dierks, K.; Bocelli, G.; Betzel, C. *J Cryst Growth* 2004, 263, 517.
5. Kunieda, K.; Seiki, T.; Nkatani, S.; Wakabayashi, M.; Shiro, T.; Inoue, K.; Sougawa, M.; Kimura, R.; Harada, K. *Br J Cancer* 1993, 67, 668.
6. Yamaguchi, I.; Lizuka, S.; Osaka, A.; Monma, H.; Tanaka, K. *Colloids Surf A* 2003, 214, 111.
7. Mukherjee, D. P.; Tunkle, A. S.; Roberts, R. A.; Clavenna, A.; Rogers, S.; Smith, D. *J Biomed Mater Res B: Appl Biomater* 2003, 67, 603.
8. Chen, F.; Cheng Wang, Z.; Lin, C. *J Mater Lett* 2002, 57, 858.
9. Ito, M.; Hidaka, Y.; Nakajima, M.; Yagasaki, H.; Kafrawy, A. H. *J Biomed Mater Res* 1999, 45, 204.
10. Maruyama, M.; Ito, M. *J Biomed Res* 1996, 32, 527.
11. Kong, L.; Gao, Y.; Cao, W.; Gong, Y.; Zhao, N.; Zhang, X. *J Biomed Mater Res A* 2005, 75, 275.
12. Wu, Y.; Seo, T.; Sasaki, T.; Irie, S.; Sakurai, K. *Carbohydr Polym* 2006, 63, 493.
13. Hirano, S.; Yamaguchi, Y.; Kamiya, M. *Carbohydr Polym* 2002, 48, 203.
14. Di Colo, G.; Zambito, Y.; Burgalassi, S.; Nardini, I.; Saettone, M. F. *Int J Pharm* 2004, 273, 37.
15. Toyama, T.; Dokushima, T.; Yasue, T.; Arai, Y. *Inorg Mater* 1998, 5, 479.
16. Qu, X.; Wirsén, A.; Albertsson, A. C. *Polymer* 2000, 41, 4841.
17. Neto, C. G. T.; Giacometti, J. A.; Job, A. E.; Ferreira, F. C.; Fonseca, J. L. C.; Oereira, M. R. *Carbohydr Polym* 2005, 62, 1.
18. Zhu, H.; Ji, J.; Lin, R.; Gao, C.; Feng, L.; Shen, J. *J Biomed Mater Res* 2002, 62, 332.